Application of Heterogeneous Adsorbents in Removal of Dimethyl Phthalate: Equilibrium and Heat

Jun Wu and Zhengwen Xu
State Key Laboratory of Pollution Control and Resources Reuse, Nanjing University, Nanjing 210093, P.R. China

Weiming Zhang
State Key Laboratory of Pollution Control and Resources Reuse, Nanjing University, Nanjing 210093, P.R. China, and
National Engineering Research Center for Organic Pollution Control and Resources Reuse, Nanjing 210046, P.R. China

Lu Lv
School of the Environment, Nanjing University, Nanjing 210093, P.R. China, and
State Environmental Protection Engineering Center for Organic Chemical Industrial Waste Water Disposal and Resources Reuse, Nanjing 210046, P.R. China

Bingcai Pan, Guangze Nie, Minghui Li, and Qiong Du
State Key Laboratory of Pollution Control and Resources Reuse, Nanjing University, Nanjing 210093, P.R. China

DOI 10.1002/aic.12175

Aminated resin (NDA-101) and oxidized resin (NDA-702) were synthesized to remove Dimethyl phthalate (DMP) from the contaminated water. The equilibrium and heat properties in the course of adsorption process were examined and compared with two commercial heterogeneous adsorbents, namely an acrylic ester resin (Amberlite XAD-7) and a coal-based granular activated carbon (AC-750). The associated equilibrium isotherms can be well fitted by Freundlich equation and the adsorption capacities for DMP followed the order: NDA-702 > NDA-101 > AC-750 > XAD-7. The surface of XAD-7 was demonstrated to be relatively homogeneous through surface energy heterogeneity analysis, offering the sole hydrogen bonding interaction. Contrarily, heterogeneous surface of oxidized resins NDA-702 and the aminated resins NDA-101 exhibited a promising adsorption capacity and affinity toward DMP probably derived by multiple hydrogen bonding, π–π stacking, and micropore filling interactions. © 2010 American Institute of Chemical Engineers *AIChE J*, 56: 2699–2705, 2010
Keywords: dimethyl phthalate, resins, heterogeneous surface, adsorption, model

Introduction

Phthalates have been widely used as an important additive to give improved flexibility, extensibility, and workability in plastic industrial processes for a long time. For example, dimethyl phthalate ester (DMP) is typically used in cellulose

---

Additional Supporting Information may be found in the online version of this article.

Correspondence concerning this article should be addressed to W. Zhang at wmzhang@nju.edu.cn or L. Lv at esellu@nju.edu.cn.

Table 1. Main Properties of Adsorbents

Adsorbent	CPS	AC-750	NDA-101	NDA-702	XAD-7
Surface polarity	Nonpolar	Polar	Moderate	Moderate	Polar
BET surface area [m^2/g (dry)]	21	749	845	804	519
Micropore volume [cm^3/g (dry)]	–	0.22	0.26	0.22	0.02
Average pore diameter (nm)	16.5	2.2	2.4	2.9	7.4
Particle size (mm)	0.4–0.8	0.4–0.8	0.4–0.8	0.4–0.8	0.4–0.8
Residual chlorine content [mmol/g (dry)]	5.0	–	0.18	0.8	–
Tertiary amino group [mmol/g (dry)]	–	–	0.14	–	–
Oxygen content (%)	–	1.4	–	2.9	27.8

ester-based plastics, such as cellulose acetate and butyrate. They are considered to be a ubiquitous pollutant in aquatic environments (around 100 μg/L)[1–4] because large quantities of DMP are released into the environment in their whole life time. Because of their endocrine disrupting, carcinogenic, or xenoestrogenic properties,[5–9] DMP is listed as one of the highest priority pollutants by the environment authorities in US and China. Thus, it is critical to effectively and economically remove phthalates from the aquatic environment. Various processes have been used to remove or degrade phthalates from surface water or industrial wastewater.[10,11] Among the most common treatment methods, either aerobic or anerobic processes require a relatively long time to render the phthalates harmless because the half-lives for the degradation of the phthalates needs from 1 day to 2 weeks in natural waters.[12–14] However, for the industrial wastewater containing DMP with considerably high concentrations (around 100 mg/L),[15] adsorption might be one of the most effective technologies to separate and even recover DMP from the wastewaters.[16–18]

More recently, polymeric resins have attracted extensive interest for removal of organic compounds from industrial effluents[19] because of high adsorption capacity, excellent adsorption selectivity, strong mechanical property, and good regenerability under mild conditions.[20,21] In general, chemical modification of polymeric resins was used to obtain larger adsorption capacity and better selectivity for a specific organic pollutant by introducing some special functional groups.[22–25] The adsorption thermodynamic aspects, including adsorption isotherm, adsorption enthalpy, adsorption entropy, and adsorption Gibbs free energy as well, of the target pollutants can be of great significance to help elucidating the underlying mechanisms. For an adsorbent with surface-energy heterogeneity, both the adsorption selectivity and the absolute value of adsorption enthalpy can usually decrease with the increase of the adsorbate loading fractions. Although lots of studies on determination of the adsorption isotherm and adsorption enthalpy[26,27] were reported, there is little knowledge on the quantitative effects of the resin surface-energy heterogeneity and the adsorbate–adsorbate interaction on the adsorption properties.[28–31]

In the present work, two types of chemically modified resins (NDA-101 with amino group and NDA-702 with hydroxyl group) were developed to mimic the multiple weak adsorbent–adsorbate interactions (hydrogen bonding, π–π stacking, and micropore filling together) on DMP adsorption. The commercial acrylic ester resin (Amberlite XAD-7) and coal-based granular activated carbon (AC-750) were selected for the comparative purpose. On the basis of the adsorption isotherms, adsorption enthalpy, adsorption Gibbs free energy, and adsorption entropy are calculated, respectively. Furthermore, the surface-energy heterogeneity of adsorbents as well as the adsorbate–adsorbate interaction on adsorbents was quantitatively explored by using Do's model.

Materials and Methods

Materials

Macroporous cross-linked chloromethylated poly(styrene-*co*-divinylbenzene) (CPS) beads were obtained from Langfang Electrical Resin (Hebei province, China), its crosslinking degree was 8%, and chlorine content was about 3.8 mmol/g (dry). The acrylic ester resin Amberlite XAD-7 was provided by Rohm and Haas (Philadelphia), and a coal-based granular activated carbon AC-750 was purchased from Shanghai reagent station (Shanghai, China). Detailed physiochemical properties of the adsorbents used in this study are presented in Table 1.

Acetone, methanol, iron chloride, dimethylamine aqueous solution (the content of dimethylamine was 30%), nitrobenzene, and DMP are of analytical grade and were also purchased from Shanghai reagent station (Shanghai, China) and used without further purification.

Synthesis of NDA-702 and NDA-101 resins

A Scheme of this experimentation is available in Scheme 1S of Supporting Information.[32] To remove residual nitrobenzene and other impurities left in the pore space of resins, the resin particles of NDA-702 and NDA-101 were finally subjected to rinsing in column with methanol/2 mol/L HCl solution (1:1 of volume ratio) and ethanol, respectively, till the effluent was transparent. Before use, all the adsorbents were packed in a column and first rinsed with 10 bed volumes (BV) of 0.01 M HCl, followed by DI washing until neutral pH. Then, the column was subjected to basic flushing by introducing 10 BV of 0.01 M NaOH and again DI flushing to neutral pH. Finally, they were extracted with ethanol for 4 h in a soxleth apparatus and vacuum desiccated at 325 K for 8 h before use. The compensating ions of NDA-101 and NDA-702 are sodium and hydroxyl, respectively.

Table 2. Isotherm Parameters of DMP Adsorption onto AC-750, NDA-101, NDA-702, and XAD-7 at Different Temperatures

		Freundlich			Langmuir		
Adsorbent	T (K)	K_F	n	R^2	K_L (L/mg)	q_m [mg/g (dry)]	R^2
AC-750	293	104 ± 0.35	5.402 ± 0.130	0.999	0.129 ± 0.097	286.8 ± 7.15	0.762
	303	82.8 ± 0.28	4.928 ± 0.187	0.997	0.160 ± 0.113	247.6 ± 1.10	0.767
	313	70.6 ± 0.97	4.665 ± 0.236	0.994	0.113 ± 0.069	230.3 ± 8.98	0.784
NDA-101	293	147 ± 0.40	5.035 ± 0.228	0.996	0.156 ± 0.088	417.0 ± 3.93	0.874
	303	115 ± 0.69	4.317 ± 0.352	0.986	0.088 ± 0.038	407.8 ± 9.33	0.916
	313	90.2 ± 0.41	3.759 ± 0.201	0.994	0.061 ± 0.023	396.2 ± 8.06	0.929
NDA-702	293	193 ± 0.80	5.778 ± 0.249	0.997	0.551 ± 0.362	447.7 ± 6.92	0.854
	303	165 ± 0.57	5.203 ± 0.226	0.996	0.265 ± 0.152	436.3 ± 3.88	0.878
	313	141 ± 0.00	4.900 ± 0.211	0.996	0.156 ± 0.085	411.5 ± 2.53	0.879
XAD-7	293	13.2 ± 0.57	2.246 ± 0.109	0.994	0.009 ± 0.001	234.7 ± 1.84	0.989
	303	7.46 ± 0.29	1.932 ± 0.117	0.991	0.006 ± 0.001	233.3 ± 2.02	0.994
	313	5.45 ± 0.75	1.808 ± 0.081	0.995	0.004 ± 0.001	228.3 ± 8.16	0.990

Batch adsorption experiments

Equilibrium adsorption experiments were carried out at 293 K, 303 K, and 313 K in 100-mL glass flasks. Adsorbent particles (0.025 g) were introduced to a 50 mL aqueous solution containing known DMP concentrations. The flask was then transferred to a G 25 model incubator shaker with thermostat (New Brunswick Scientific) and shaken under 150 rpm until the adsorption process reached equilibrium, as indicated by the preliminary kinetic study. The background solution contained 10^{-3} M KH_2PO_4 for buffering the aqueous solutions at pH 5.5–7.0. The amount of solute loaded on the resin particles was calculated by conducting a mass balance on the solute before and after the test. The control experiments were conducted using flasks prepared similarly but containing no resin for assessing loss of solutes to the flask components during adsorption tests. Results of triplicate flasks showed that the average concentrations of solution phase were within 96–100% of the respective initial concentration of the same solution analyzed similarly. Hence, compound loss was negligible.

Analysis

All the solution concentrations of DMP were analyzed spectrophotometrically using a Helious Betra UV-Vis spectrophotometer at wavelength of 228 nm. The analytical detection limit was about 0.2 mg/L DMP. Surface area and pore size distribution of adsorbents were determined by using a Micrometrics 2010C automatic analyzer (Australia). Infrared spectra of the adsorbents in the range of 650–4000 cm^{-1} were collected by a Nexus 870 FT-IR spectrometer with a pellet of powdered potassium bromide. The chlorine content was measured according to the method of Volhard.[33]

Results and Discussion

Characterization of adsorbents

Table 1 presents the typical properties of CPS, AC-750, NDA-101, NDA-702, and XAD-7. It can be shown that AC-750, NDA-101, and NDA-702 have similar BET surface area and micropore structures, but quite different chemical composition. The BET surface area and micropore structure of XAD-7 are much less than those of AC-750, NDA-101, and NDA-702. Thanks to IR experiments (spectra are given in Figure 1S of Supporting Information), the presence of tertiary amino group on NDA-101, of carbonyl and hydroxyl groups on polymer matrix of NDA-702 and of carbonyl, acetyl, and ester groups characteristic of the acrylic ester matrix of XAD-7[34] were detected.

Adsorption isotherms

Adsorption isotherms of DMP are represented by the Langmuir model (Eq. 1) and Freundlich model (Eq. 2):

$$q_e = \frac{K_L q_m C_e}{1 + K_L C_e} \tag{1}$$

$$q_e = K_F C_e^{1/n} \tag{2}$$

where q_e [mmol/g (dry)] is the equilibrium adsorption capacity, C_e (mmol/L) represents the solute concentration in equilibrium, q_m [mmol/g (dry)] is the maximum adsorption capacity [mmol/g (dry)], K_L is a binding constant (L/mmol), K_F is a characteristic parameter and an indicator of adsorption capacity, whereas n refers to an adsorption intensity and is an indicator of the favorableness of the adsorbent–adsorbate system. All these parameters are listed in Table 2 and isotherms could be found in Figure 2S of Supporting Information.

First, regression coefficients listed in Table 2 indicated that the adsorption isotherms can be much better fitted with the Freundlich model than with the Langmuir one. K_F values are observed in the following sequence as NDA-702 $>$ NDA-101 $>$ AC-750 $\gg$ XAD-7. The significant higher adsorption capacity of NDA-702, NDA-101, and AC-750 than XAD-7 presumably resulted from their higher micropore volume, where DMP can be intensively adsorbed by micropore filling mechanism. Second, the phenyl ring on AC-750, NDA-702, and NDA-101 is also favorable to increase the adsorption capacity and affinity of the aromatic ring on DMP molecule by the proposed π–π interaction that can not be established in XAD-7 because of its lack of phenyl ring. Third, the hydrogen atom of the

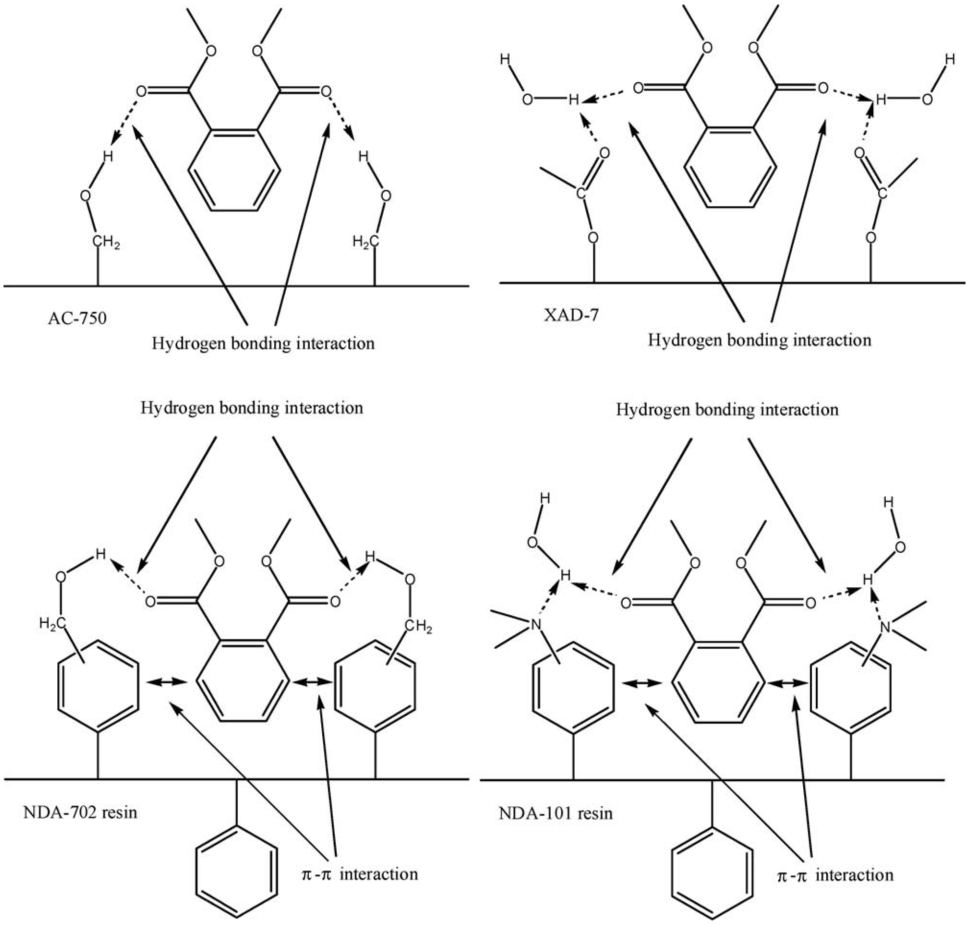

Figure 1. Schemes for the proposed adsorption driving force of DMP onto (a) AC-750, (b) NDA-101, (c) NDA-702, and (d) XAD-7.

hydroxyl group on NDA-702 and AC-750 can directly act as hydrogen bonding acceptor and form hydrogen bonding with the oxygen atom of the ester group of DMP molecules. Besides, the nitrogen atom of the amino group on NDA-101 and the oxygen atom of the carbonyl group on XAD-7 might also play a role of hydrogen bonding donator and can form hydrogen bonding with the oxygen atom of the ester group of DMP through the water molecules (in Figure 1).[35–37]

Adsorption selectivity

To understand and quantify the adsorption selectivity of the two chemical modified polymer resins (NDA-702 and NDA-101) and the two comparative adsorbents (XAD-7 and AC-750), the distribution ratio K_d (in L/g) was determined by the following equation[38]:

$$K_\mathrm{d} = \frac{\text{mg of DMP}/1\text{ g of dry resin}}{\text{mg of DMP}/1\text{ L of solution}} \tag{3}$$

At low adsorbate fractional loading (see Figure 3S of Supporting Information), K_d values of DMP adsorption decrease as NDA-702 $>$ AC-750 $>$ NDA-101 $\gg$ XAD-7, which helps NDA-702 and NDA-101 to selectively removing DMP from contaminated water dramatically. The much larger selectivity of NDA-702, AC-750, and NDA-101 for DMP is probably due to its particular multiple adsorption forces of hydrogen bonding, micropore filling, and π–π taking interactions. XAD-7 reasonably showed the lowest adsorption affinity to DMP molecule due to the sole adsorbent–adsorbate interaction of hydrogen bonding interaction. It is also shown in Figure 3S of Supporting Information that the adsorption selectivity of NDA-702 and NDA-101 decreases sharply with an increasing adsorbate loading fraction (θ), suggesting their much heterogeneous nature.

Effect of temperature and thermodynamic analysis

Comparison of the results obtained at three different temperatures for AC-750, NDA-702, NDA-101, and XAD-7 shows that the lower temperature is favorable for DMP adsorption, indicating an exothermic nature of the adsorption processes (see Figure 2S of Supporting Information). The lower the free energy change (ΔG), enthalpy change (ΔH), and entropy change (ΔS) during adsorption process were calculated by the following equations.[39]

$$\Delta G = -nRT \tag{4}$$

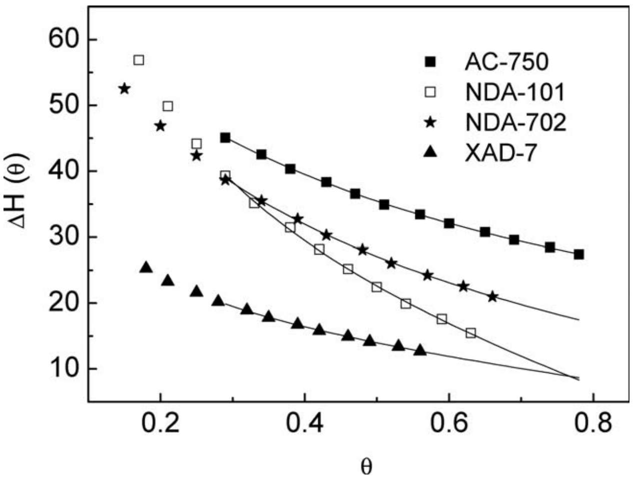

Figure 2. Isosteric enthalpy dependence on fractional loading of DMP adsorption and the fitted curves.

$$\ln C_e = \ln K + (-\Delta H/RT) \qquad (5)$$

$$\Delta S = (\Delta H - \Delta G)/T \qquad (6)$$

where n is the characteristic constant in Freundlich equation, R is the universal gas constant (8.314 kJ/mol/K), T is the temperature (K), and K is a constant. From van't Hoff equilibrium equation of Eq. 5, ΔH can be figured out from the isosters, plot of ln C_e vs. $1/T$ (Figure 4S of Supporting Information). These isosters are straight lines and ΔH can be calculated from their slope. Thermodynamic parameters of DMP adsorption are listed in Table 1S of Supporting Information.

The negative values of ΔH, ΔG, and ΔS indicate that adsorption processes of DMP onto the four adsorbents are exothermic and spontaneous. They were mainly driven by enthalpy change. Different ΔH values at different adsorbate loading levels indicated the heterogeneous nature of the adsorbent surface. Initially, DMP molecules favorably adsorb on the adsorbent surface at high-energy sites, and the absolute value of ΔH is largest among the whole adsorption process. With increasing adsorbate loading level, the adsorbent surface with high-energy sites has been occupied gradually, and the subsequent DMP molecules have to adsorb on the adsorbent surface at relatively low-energy sites, so that the absolute values of ΔH become less than the initial one.[23,28]

Table 1S of Supporting Information also presents that at the same temperature and adsorbate loading level, compared to XAD-7, the larger losses of enthalpy and entropy (ΔH and ΔS) about DMP adsorption onto AC-750, NDA-101, and NDA-702 supports the proposed adsorption mechanism discussed in the previous section: DMP adsorption on AC-750, NDA-101, and NDA-702 is driven by hydrogen bonding, micropore filling, and π–π taking interactions together whereas the one on XAD-7 is due to the sole hydrogen bonding interaction.

Surface energy heterogeneity of resins

Do's model was adopted to clarify the surface energy heterogeneity of adsorbents.[23,28,40] It takes the isosteric adsorption enthalpy change as a function of the adsorbate fractional loading:

$$\Delta H(\theta) = \Delta H_0(1 - \alpha\beta\theta/[1 + (\beta - 1)\theta]) + \mu\theta \qquad (7)$$

where $\Delta H(\theta)$ is the isosteric adsorption enthalpy change at the loading of θ on adsorbent, ΔH_0 is the enthalpy change at zero loading, β is the pattern parameter, μ is the adsorbate–adsorbate interaction energy between adsorbed molecules, and α is defined as:

$$\alpha = \delta H/\Delta H_0 \qquad (8)$$

where α represents the extent of the surface energy heterogeneity of adsorbent. The larger the α value is, the greater the extent of surface energy heterogeneity is, and δH reflects the enthalpy change with the loading fraction from 0 to 1.

As for DMP adsorption, $\Delta H(\theta)$ can be obtained directly from the adsorption isoster (see Figure 4S of Supporting Information), and θ can be figured out from the adsorption capacity corresponding to $\Delta H(\theta)$ and the maximum adsorption capacity from the extrapolation of the well fitted isotherm. Figure 2 shows the $\Delta H(\theta)$ dependence on θ. The surface energy heterogeneity of adsorbent was calculated by fitting the measured isosteric enthalpy change to Eq. 7 with nonlinear method, and the four parameters, ΔH_0, α, β, and μ, are gathered in Table 3. The standard errors and dependence values listed in Table 3 indicate that the fitted results are reliable, which means Do's model can describe the surface energy heterogeneity of the adsorbents efficiently.

As seen in Table 3, the extrapolated initial adsorption enthalpy changes (ΔH_0) of DMP adsorption onto AC-750, NDA-702, and NDA-101 are larger than those on XAD-7, and, thus, reinforces the hypothesis according to which DMP adsorption onto AC-750 and the chemical modified resins NDA-702 and NDA-101 is driven by multiple physical forces including hydrogen bonding, micropore filling, and π–π staking interactions, as depicted in Figure 1. The α values of XAD-7 slightly lower than those of AC-750, NDA-702, and NDA-101, implying the more homogeneous surface of XAD-7. It is probably due to the sole hydrogen bonding interaction between XAD-7 and DMP. Compared to the initial adsorption

Table 3. Nonlinear Fitting Results of Isosteric Adsorption Enthalpy and Some Other Characteristic Parameters

Resin	ΔH_0	α	β	μ	R^2
AC-750	70.31 ± 4.99	0.728 ± 0.200	2.61 ± 1.151	4.30 ± 15.92	0.9997
NDA-101	144.5 ± 26.78	0.808 ± 0.011	11.89 ± 5.004	−28.38 ± 6.29	0.9998
NDA-702	81.88 ± 3.73	0.739 ± 0.060	4.85 ± 1.144	−9.23 ± 6.78	0.9998
XAD-7	62.21 ± 28.79	0.719 ± 0.083	15.92 ± 16.473	−12.25 ± 4.01	0.9995

enthalpy changes (ΔH_0), all the β values are almost zero, indicating that this pattern parameter is independent of adsorbate. Compared to the initial adsorption enthalpy changes (ΔH_0), the μ values for all the test adsorbents are almost zero, suggesting that the adsorbate–adsorbate interaction between adsorbed molecules is not as important as the adsorbate–adsorbent interaction in such adsorption systems.

Conclusions

Compared to commercial acrylic ester resin XAD-7 and coal-based granular activated carbon AC-750, the two chemically modified resins, namely NDA-101 with amino group and NDA-702 with hydroxyl group, were developed and exhibited excellent adsorption capacity toward DMP from the contaminated waters. The Freundlich models can be used to well simulate the adsorption isotherms. The adsorption, mainly driven by enthalpy change, is shown to be an exothermic and spontaneous process.

The four adsorbents exhibit different surface energy heterogeneities for DMP adsorption in aqueous solution and can be quantitatively described by Do's model. Analysis of adsorption mechanism suggests that multiple driving forces of hydrogen bonding, micropore filling, and π–π taking interactions are involved for the adsorption of DMP onto the two chemically modified resins.

Acknowledgments

This research was financially funded by National Natural Science Funding of P.R. China (Grant No. 20744005) and Natural Science Funding of Jiangsu province (Grant BK 2009251).

Literature Cited

1. Xu N, Ni JR, Sun WL, Borthwick AGL. Role of dissolved organic carbon in the cosorption of copper and phthalate esters onto Yellow River sediments. *Chemosphere.* 2007;69:1419–1427.
2. Mackintosh CE, Maldonado JA, konomou MGI, Gobas FAPC. Sorption of phthalate esters and PCBs in a marine ecosystem. *Environ Sci Technol.* 2006;40:3481–3488.
3. Kapanen A, Stephen JR, Bruggemann J, Kiviranta A, White DC, Itavaara M. Diethyl phthalate in compost: ecotoxicological effects and response of the microbial community. *Chemosphere.* 2007;67:2201–2209.
4. Pan GW, Hanaoka T, Yoshimura M, Zhang SJ, Wang P, Tsukino H, Inoue K, Nakazawa H, Tsugane S, Takahashi K. Decreased serum free testosterone in workers exposed to high levels of di-*n*-butyl phthalate (DBP) and di-2-ethylhexyl phthalate (DEHP): a cross-sectional study in China. *Environ Health Persp.* 2006;114:1643–1648.
5. Silva MJ, Samandar E, Reidy JA, Hauser R, Needham LL, Calafat AM. Metabolite profiles of di-*n*-butyl phthalate in humans and rats. *Environ Sci Technol.* 2007;41:7576–7580.
6. EPA. *Effluent Guidelines and Standards: Organic Chemicals, Plastics, and Synthetic Fibers.* 40 CFR Part 414. Washington, DC: Environmental Protection Agency, 1988.
7. EPA of China. *Integrated Wastewater Discharge Standard (GB8978-1996).* Beijing: State Environmental Protection Agency of China, 1996.
8. Meeker JD, Calafat AM, Hauser R. Di(2-ethylhexyl) phthalate metabolites may alter thyroid hormone levels in men. *Environ Health Persp.* 2007;115:1029–1034.
9. Itoh H, Yoshida K, Masunaga S. Quantitative identification of unknown exposure pathways of phthalates based on measuring their metabolites in human urine. *Environ Sci Technol.* 2007;41:4542–4547.
10. Patnaik P, Yang M, Powers E. Kinetics of phthalate reactions with ammonium hydroxide in aqueous matrix. *Water Res.* 2001;35:1587–1591.
11. Yuan BL, Lia XZ, Grahamc N. Aqueous oxidation of dimethyl phthalate in a Fe(VI)-TiO_2-UV reaction system. *Water Res.* 2008;42:1413–1420.
12. Liang DW, Zhang T, Fang HHP. Anerobic degradation of dimethyl phthalate in wastewater in a UASB reactor. *Water Res.* 2007;41:2879–2884.
13. Wu DL, Hu BL, Zheng P, Qaisar M. Anoxic biodegradation of dimethyl phthalate (DMP) by activated sludge cultures under nitrate-reducing conditions. *J Environ Sci China.* 2007;19:1252–1256.
14. Roslev P, Vorkamp K, Aarup J, Frederiksen K, Nielsen PH. Degradation of phthalate esters in an activated sludge wastewater treatment plant. *Water Res.* 2007;41:969–976.
15. Bajt O, Mailhot G, Bolte M. Degradation of dibutyl phthalate by homogeneous photocatalysis with Fe(III) in aqueous solution. *Appl Catal B: Environ.* 2001;33:239–248.
16. Yoshida H, Galinada WA. Equilibria for adsorption of phosphates on OH-type strongly basic ion exchanger. *AIChE J.* 2002;48:2193–2202.
17. Li WL, Liu QF, Xing JM, Gao HS, Xiong XC, Li YG, Li X, Liu HZ. High-efficiency desulfurization by adsorption with mesoporous aluminosilicates. *AIChE J.* 2007;53:3263–3268.
18. Mohan SV, Shailaja S, Krishna MR, Sarma PN. Adsorptive removal of phthalate ester (di-ethyl phthalate) from aqueous phase by activated carbon: a kinetic study. *J Hazard Mater.* 2007;146:278–282.
19. Pan BC, Du W, Zhang WM, Zhang X, Zhang QR, Pan BJ, Lv L, Zhang QX, Chen JL. Improved adsorption of 4-nitrophenol onto a novel hyper-cross-linked polymer. *Environ Sci Technol.* 2007;41:5057–5062.
20. Fontanals N, Marce RM, Borrull F. Improved polymeric materials for more efficient extraction of polar compounds from aqueous samples. *Curr Anal Chem.* 2006;2:171–179.
21. Hong CH, Zhang WM, Pan BC, Lv L, Han YZ, Zhang QX. Adsorption and desorption hysteresis of 4-nitrophenol on a hyper-cross-linked polymer resin NDA-701. *J Hazard Mater.* 2009;168:1217–1222.
22. Zhang WM, Hong CH, Pan BC, Zhang QJ, Jiang PJ, Jia K. Sorption enhancement of 1-naphthol onto a hydrophilic hyper-cross-linked polymer resin. *J Hazard Mater.* 2009;163:53–57.
23. Huang J, Huang K, Liu S, Luo Q, Xu M. Adsorption properties of tea polyphenols onto three polymeric adsorbents with amide group. *J Colloid Interface Sci.* 2007;315:407–414.
24. Ming ZW, Long CJ, Cai PB, Xing ZQ, Zhang B. Synergistic adsorption of phenol from aqueous solution onto polymeric adsorbent. *J Hazard Mater.* 2006;128:123–129.
25. Lee TK, Ryoo SJ, Byun JW, Lee SM, Lee YS. Preparation of core-shell-type aminomethyl polystyrene resin and characterization of its functional group distribution. *J Comb Chem.* 2005;7:170–173.
26. Bilgili MS. Adsorption of 4-chlorophenol from aqueous solutions by xad-4 resin: isotherm, kinetic, and thermodynamic analysis. *J Hazard Mater.* 2006;137:157–164.
27. Danko B, Trochimczuk AW, Samczyński Z, Hamerska-Dudra A, Dybczyński RS. An attempt to differentiate the affinity of individual lanthanides to the resin using temperature driven swelling of the thermosensitive copolymer of *N*-isopropylacrylamide and 2-(methacryloyloxy)ethyl phosphate—thermodynamic studies. *React Funct Polym.* 2007;67:1651–1659.
28. Do DD, Do HD. A new adsorption isotherm for heterogeneous adsorbent based on the isosteric heat as a function of loading. *Chem Eng Sci.* 1997;52:297–310.
29. Ramirez D, Qi SY, Rood MJ. Equilibrium and heat of adsorption for organic vapors and activated carbons. *Environ Sci Technol.* 2005;39:5864–5871.
30. Garcia-Zubiri IX, Gonzalez-Gaitano G, Isasi JR. Isosteric heats of sorption of 1-naphthol and phenol from aqueous solutions by β-cyclodextrin polymers. *J Colloid Interface Sci.* 2007;307:64–70.
31. Zhang WM, Xu ZW, Pan BC, Zhang QJ, Zhang QR, Du W, Pan BJ, Zhang QX. Cooperative effect of lateral acid-base interaction on 1-naphthol/1-naphthylamine binary adsorption onto nonpolar polymer adsorbents. *Sep Purif Technol.* 2007;55:141–146.

32. Davankov VA, Tsyurupa MP. Structure and properties of hypercrosslinked polystyrene—the first representative of a new class of polymer networks. *React Polym.* 1990;13:27–42.
33. Central China Normal University. *Analytical Chemistry*, 1st ed. Beijing: People's Education Press, 1981:418.
34. Wang JT, Hu QM, Zhang BS, Wang YM. *Organic Chemistry*. Tianjing: Nankai University Press, 1998:432.
35. Wang QW, Yang YH, Gao HB. *Problems on Hydrogen Bond in Organic Chemistry*. Tianjing: Nankai University Press, 1993:5.
36. Dabrowski A. Adsorption from theory to practice. *Adv Colloid Interface Sci.* 2001;93:135–224.
37. Ersöz A, Denizli A, Sener I, Atilir A, Diltemiz S, Say R. Removal of phenolic compounds with nitrophenol-imprinted polymer based on π–π and hydrogen-bonding interactions. *Sep Purif Technol.* 2004;38:173–179.
38. Bonnesen PV, Brown GM, Alexandratos SD, Bavoux LB, Presley DJ, Patel V, Ober R, Moyer BA. Development of bifunctional anion-exchange resins with improved selectivity and sorptive kinetics for pertechnetate: batch-equilibrium experiments. *Environ Sci Technol.* 2000;34:3761–3766.
39. Gupta VK, Ali I, Saini VK. Removal of chlorophenols from wastewater using red mud: an aluminum industry waste. *Environ Sci Technol.* 2004;38:4012–4018.
40. Valenzuela-Calahorro C, Navarrete-Guijosa A, Stitou M, Cuerda-Correa EM. A comparative study of the adsorption equilibrium of progesterone by a carbon black and a commercial activated carbon. *Appl Surf Sci.* 2007;253:5274–5280.

Manuscript received Jun. 1, 2009, and revision received Dec. 4, 2009.